

Using leaf optical properties to detect ozone effects on foliar biochemistry

Elizabeth A. Ainsworth · Shawn P. Serbin ·
Jeffrey A. Skoneczka · Philip A. Townsend

Received: 27 November 2012 / Accepted: 23 April 2013 / Published online: 9 May 2013
© Springer Science+Business Media Dordrecht (outside the USA) 2013

Abstract Efficient methods for accurate and meaningful high-throughput plant phenotyping are limiting the development and breeding of stress-tolerant crops. A number of emerging techniques, specifically remote sensing methods, have been identified as promising tools for plant phenotyping. These remote sensing methods can be used to accurately and rapidly relate variations in leaf optical properties with important plant characteristics, such as chemistry, morphology, and photosynthetic properties at the leaf and canopy scales. In this study, we explored the potential to utilize optical ($\lambda = 500\text{--}2,400\text{ nm}$) near-surface remote sensing reflectance spectroscopy to evaluate the effects of ozone pollution on photosynthetic capacity of soybean (*Glycine max* Merr.). The research was conducted at the Soybean Free Air Concentration Enrichment (SoyFACE) facility where we subjected plants to ambient (44 nL L^{-1}) and elevated ozone ($79\text{--}82\text{ nL L}^{-1}$ target) concentrations throughout the growing season. Exposure to elevated ozone resulted in a significant loss of productivity, with the ozone-treated plants displaying a $\sim 30\%$ average decrease in seed yield. From leaf reflectance data, it was

also clear that elevated ozone decreased leaf nitrogen and chlorophyll content as well as the photochemical reflectance index (PRI), an optical indicator of the epoxidation state of xanthophyll cycle pigments and thus physiological status. We assessed the potential to use leaf reflectance properties and partial least-squares regression (PLSR) modeling as an alternative, rapid approach to standard gas exchange for the estimation of the maximum rates of RuBP carboxylation ($V_{c,max}$), an important parameter describing plant photosynthetic capacity. While we did not find a significant impact of ozone fumigation on $V_{c,max}$, standardized to a reference temperature of $25\text{ }^{\circ}\text{C}$, the PLSR approach provided accurate and precise estimates of $V_{c,max}$ across ambient plots and ozone treatments ($r^2 = 0.88$ and $\text{RMSE} = 13.4\text{ }\mu\text{mol m}^{-2}\text{ s}^{-1}$) based only on the variation in leaf optical properties and despite significant variability in leaf nutritional status. The results of this study illustrate the potential for combining the phenotyping methods used here with high-throughput genotyping methods as a promising approach for elucidating the basis for ozone tolerance in sensitive crops.

E. A. Ainsworth (✉) · J. A. Skoneczka
Agricultural Research Service, Global Change and
Photosynthesis Research Unit, US Department of Agriculture,
University of Illinois, Urbana-Champaign, 1201 W. Gregory
Drive, Urbana, IL 61801, USA
e-mail: lisa.ainsworth@ars.usda.gov

E. A. Ainsworth
Department of Plant Biology, University of Illinois, Urbana-
Champaign, 1201 W. Gregory Drive, Urbana, IL 61801, USA

S. P. Serbin · P. A. Townsend
Department of Forest and Wildlife Ecology, University of
Wisconsin-Madison, 226 Russell Labs, 1630 Linden Drive,
Madison, WI 53706, USA

Keywords Air pollution · Photochemical reflectance index · Photosynthesis · Remote sensing · Rubisco · Spectroscopy

Introduction

A widely recognized bottleneck in the development and breeding of stress-tolerant crops is accurate and meaningful high-throughput phenotyping (Furbank and Tester 2011; Tuberosa 2012). Near-surface remote sensing of leaf optical properties has been identified as a promising phenotyping technique (Montes et al. 2007). By monitoring the

spectral reflectance of a leaf or plant canopy, a number of physiological traits can be inferred by correlation with leaf optical properties (Curran 1989; Kokaly et al. 2009; Asner et al. 2011; Ollinger 2011). Measurements of leaf optical properties are non-destructive and rapid, taking only a few seconds, and therefore can be done in the field on a large number of individual plants. Simple spectral reflectance indices based on the ratio of reflected light in the near-infrared (NIR, 700–1,300 nm) to visible wavelengths (Vis, 400–700 nm) have been developed to predict vegetative parameters such as green biomass, leaf area index (LAI, $\text{m}^2 \text{m}^{-2}$, per horizontal datum), and photosynthetic radiation absorption (Myneni and Williams 1994; Gamon et al. 1995; Gitelson et al. 2003). Other more intricate spectral reflectance indices have been developed to assess radiation use efficiency and the water status of plant canopies (Gamon et al. 1992, 1997; Peñuelas et al. 1993, 1995). Spectral reflectance indices have also been demonstrated to be effective in application as breeding tools or to identify nutrient or water stressed crops (e.g., Osborne et al. 2002; Babar et al. 2006).

Recently, novel statistical methods have been developed to determine photosynthetic properties of leaves from reflectance information in the Vis, NIR, and short-wave infrared (SWIR, 1,300–2,500 nm) spectral regions. In particular, partial least-squares regression (PLSR) methods allow empirical estimation of parameters that are mechanistically linked to the biochemistry of carbon assimilation, specifically the maximum carboxylation rate of ribulose biphosphate (RuBP) carboxylation by Rubisco ($V_{c,\max}$) and the maximum rate of RuBP regeneration (J_{\max} ; Doughty et al. 2011; Serbin et al. 2012). These two leaf traits ($V_{c,\max}$ and J_{\max}) largely determine the photosynthetic performance of a leaf, and are used in a widely adopted and validated biochemical model of photosynthesis (Farquhar et al. 1980; Farquhar and von Caemmerer 1982), which has been scaled to the canopy and ecosystem levels (e.g., Chen et al. 1999; Baldocchi and Wilson 2001; Medvigy et al. 2009). The use of spectral measurements to estimate these metabolic properties has opened a wide range of applications for rapid characterization of plant properties. The combination of such phenotyping methods with high-throughput genotyping offers a promising approach for elucidation of the underlying genetic basis of complex plant traits related to photosynthetic production (Montes et al. 2007).

Ozone is a dynamic secondary pollutant, which enters leaves through the stomata, generates other reactive oxygen species and causes oxidative stress (Fiscus et al. 2005). This damage in turn decreases photosynthesis, plant growth, biomass accumulation, and crop yield (Fuhrer et al. 1997; Fumigalli et al. 2001; Ashmore 2005; Fiscus et al. 2005; Ainsworth et al. 2012), with cumulative exposure to

concentrations over 40 nL L^{-1} causing linear decreases in crop production (Fuhrer et al. 1997; Mills et al. 2007; Betzelberger et al. 2012). Current concentrations of ozone cause wide-spread visual damage to leaves of natural and managed species (Mills et al. 2011). However, even in the absence of visual symptoms, ozone can decrease rates of photosynthesis (Biswas et al. 2008). In such cases, the loss of Rubisco activity is thought to be the primary cause of decreased carbon assimilation (Farge and Long 1999). Although the impact of ozone damage on crops is substantial, with global estimates of lost profit between \$14 and \$26 billion (Van Dingenen et al. 2009), large-scale breeding or biotechnological efforts to improve ozone tolerance in sensitive crops have yet to be initiated in the industrial sector (Ainsworth et al. 2008). This is in part because ozone is a dynamic air pollutant, with variable concentrations from day to day, season to season, and year to year, but also because of the difficulty in screening germplasm for ozone tolerance. Foliar injury has been used to assess ozone tolerance in crops (Heagle and Letchworth 1982; Burkey and Carter 2009); however, injury from ozone that ultimately decreases productivity is not always visible on leaves, and therefore developing other methods of screening is an important first step toward selecting for ozone tolerance.

Previous studies have used remotely sensed indices to monitor the effects of ozone (reviewed by Meroni et al. 2009), and have shown that changes in photochemical reflective index (PRI, Gamon et al. 1992; 1997) in plants exposed to elevated ozone precede visual damage to leaves. PRI provides an indication of de-epoxidation of the xanthophyll pigments, hence diversion of energy to nonphotochemical quenching (NPQ), and is strongly correlated with light-use efficiency (Gamon et al. 1997; Grace et al. 2007; Coops et al. 2010). The decrease in PRI in plants exposed to elevated ozone indicates increased NPQ and an increase in the de-epoxidation state of the xanthophylls pool, which has been supported by biochemical analyses (Castagna et al. 2001; Ranieri et al. 2001). Previous analyses of the spectral properties of soybean leaves (Campbell et al. 2007) and canopies (Gray et al. 2010) have also indicated that PRI is a promising index for assessing ozone sensitivity.

In this study, we examined the potential to use leaf reflectance data, spectral indices and hyperspectral modeling to assess ozone damage to photosynthesis in 11 diverse genotypes of soybean (*Glycine max* Merr.; Table 1) grown in the field under open-air conditions. We chose soybean because it is particularly sensitive to ozone (Mills et al. 2007; Betzelberger et al. 2012) and because the photosynthetic and growth response of soybean to elevated ozone concentrations has been examined in detail. According to a recent compilation of crop response studies using the metric accumulated exposure over a threshold of 40 nL L^{-1} (AOT40), the critical level for damage to

Table 1 List and description of soybean genotypes used in the study

| Genotype | Release date | Maturity group | Pedigree |
|---------------|--------------|----------------|------------------------|
| A.K. (Harrow) | 1950 | III | Selected by A.K. |
| Cumberland | 1977 | III | Corsoy × Williams |
| Dunfield | 1954 | III | Selected from PI 36846 |
| Dwight | 1997 | II | Jack × A86-303014 |
| Jogun | 1951 | III | Selected from PI 87615 |
| Lincoln | 1954 | III | Mandarin × Manchu |
| Pana | 1997 | III | Jack × Asgrow A3205 |
| Pella | 1979 | III | L66L-137 × Calland |
| PI 88788 | 1930 | III | |
| Richland | 1954 | II | Selected from PI 70502 |
| Williams 82 | 1980 | III | Williams (7) × Kingwa |

soybean or the level which causes a 5 % reduction in yield, is 4.3 ppm h over 3 months (Mills et al. 2007). This concentration is regularly exceeded today in many soybean-growing regions, including the Midwest U.S. Previous research has shown that while the maximum potential photosynthetic capacity was not consistently altered by a 25–50 % increase in ozone concentration, ozone accelerated the process of senescence leading to decreased photosynthetic capacity in aging leaves and canopies (Morgan et al. 2004; Betzelberger et al. 2010). In the current study, we also tested whether leaf reflectance spectra could be used to accurately predict $V_{c,max}$ in soybean exposed to ambient and elevated ozone concentrations. While infrared gas exchange analysis is commonly used to accurately estimate $V_{c,max}$ (Long and Bernacchi 2003), measurements are time and labor-intensive and ill-suited to large-scale screening. Therefore, development of techniques to estimate $V_{c,max}$ from spectral data may be particularly useful for screening for ozone or other stress tolerance.

Materials and methods

Experimental site

Soybeans were exposed to elevated ozone concentrations at the Soybean Free Air Concentration Enrichment (SoyFACE) facility located on 32 ha near Champaign, IL, USA (40°02'N, 88°14'W, 228 m above sea level; <http://www.igb.illinois.edu/soyface/>). Detailed descriptions of the facility have been published previously (Rogers et al. 2004; Morgan et al. 2004; Betzelberger et al. 2010). In 2011, the ozone experiment consisted of eight ambient and eight elevated 20-m diameter octagonal plots. Plots were fumigated with air enriched with ozone (100 nL L⁻¹ target) from 9:00 to 17:00, except when leaves were wet or there was insufficient wind

for accurate fumigation. The ambient 8 h ozone concentration over the 2011 growing season was 44 nL L⁻¹, and the 8 h average concentration in the FACE plots ranged from 79 to 82 nL L⁻¹ (Fig. 1). One-minute average concentrations were within 20 % of the 100 nL L⁻¹ target for 88–93 % of the time.

Eleven soybean genotypes were investigated in this study (Table 1). Two genotypes, Dwight and Pana, were planted in ambient and elevated ozone plots in a replicated design ($N = 8$). Genotypes were planted in two row plots, 1.5 m long, with 0.76 m row spacing. Nine additional genotypes, A.K. (Harrow), Cumberland, Dunfield, Jogun, Lincoln, Pella, PI 88788, Richland, and Williams 82, were planted in three elevated ozone plots ($N = 3$) in similar 1.5 m double row plots (0.76 m row spacing). Ambient plots for these nine genotypes were planted in plots of four 2.43 m rows with 0.76 m row spacing ($N = 1$). The ambient plots were located in the field >100 m from the FACE plots to avoid cross-fumigation.

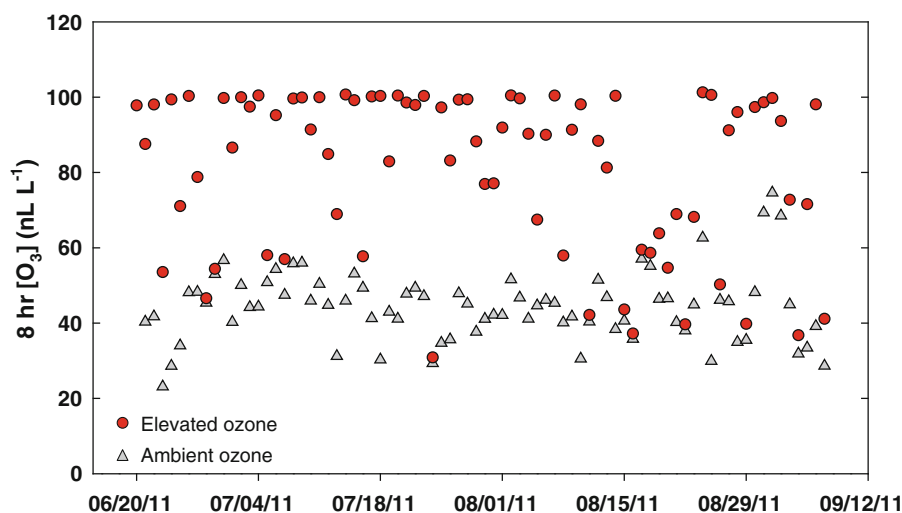
Leaf gas exchange

The response of photosynthesis (A) to intercellular CO₂ concentration (c_i) was measured in the field with a portable infrared gas analyzer (LI-6400, Li-Cor Biosciences, Lincoln, NE, USA) on two soybean genotypes, Pana and Dwight. These genotypes were used because they have been previously shown to have different sensitivities to ozone (Betzelberger et al. 2010). Gas exchange measurements were performed from 17 to 21 Aug 2011. Gas exchange was measured on a mature leaf at the top of the canopy at saturating light (2,000 $\mu\text{mol m}^{-2} \text{s}^{-1}$). Measurements were initiated at the growth CO₂ concentration (400 $\mu\text{mol mol}^{-1}$). Next, the reference CO₂ concentration was reduced stepwise to a lower concentration of 50 $\mu\text{mol mol}^{-1}$. Photosynthesis was measured at five CO₂ concentrations in order to provide the initial slope of the A/c_i response. Each stepwise measurement was completed within 1 or 2 min in order to minimize alteration of the activation state of Rubisco. Leaf temperature was measured with an infrared thermometer (Agri-Therm III, Everest Interscience, Tucson, AZ, USA) before the A/c_i curve was initiated and the block temperature was set to keep constant cuvette temperature for the subsequent measurements. Gas exchange measurements were acquired from 3 to 6 leaves per genotype from each of 4 ambient and 4 elevated ozone plots (59 A/c_i curves measured in total).

Calculation of $V_{c,max}$ from gas exchange measurements

Estimates of $V_{c,max}$ and dark respiration (R_d) were calculated by fitting the equations of Farquhar et al. (1980). We calculated the optimum $V_{c,max}$ for each measured A/c_i curve using the derivative evolution (DE) algorithm (Price

Fig. 1 Ozone concentrations measured between 9:00 to 17:00 (8 h [O₃]) in the elevated ozone plots and in the ambient air at SoyFACE during the 2011 growing season. The 8 h target concentration (100 nL L⁻¹) was attained regularly throughout the season. We did not fumigate on rainy days or days with insufficient wind speed, and so the season-long 8 h ozone concentration in the elevated ozone plots was 81 nL L⁻¹ and the ambient ozone concentration was 44 nL L⁻¹



et al. 2006) implemented in the R (R Development Core Team, 2008) package “DEoptim” (Ardia 2009) to minimize the difference between the modeled and observed photosynthetic rates to derive the optimum $V_{c,max}$ and R_d for each A/c_i curve. Michaelis–Menten constants for CO₂ (K_c) and oxygen (K_o), as well as the photosynthetic (CO₂) compensation point (Γ^*) were derived using the temperature-dependent formulae of Bernacchi et al. (2001). Our parameter optimization strategy was implemented to avoid the co-limited region of the A/c_i curve, and $V_{c,max}$ was estimated from data where $c_i < 250$ mmol mol⁻¹.

We quantified the temperature dependence of $V_{c,max}$ using a modified Arrhenius model (Medlyn et al. 2002; Dillaway and Kruger 2010):

$$V_{T_i} = V_{25} e^{\left[\frac{E_v}{R_g} \left(\frac{1}{T_{25}} - \frac{1}{T_i} \right) \right]}$$

where V_{25} is the $V_{c,max}$ at the reference temperature of 25 °C, T_{25} and T_i are temperatures in Kelvin, V_{T_i} is the $V_{c,max}$ at the measured temperature T_i , E_v is the energy of activation for RuBP carboxylation, and R_g is the ideal gas constant (8.314 J mol⁻¹ K⁻¹). Based on the $V_{c,max}$ values calculated at three to five leaf temperatures, we determined V_{25} and E_v using the “DEoptim” parameter optimization algorithm in R. For the samples included in this study, we did not observe a peaked response of $V_{c,max}$ temperature (Medlyn et al. 2002; Kattge and Knorr 2007); therefore, all temperature responses are based on the Arrhenius model described above. Estimates from individual leaves were averaged for each plot ($N = 4$), and statistical differences between genotypes and ozone treatments were calculated based on plot mean.

Leaf optical properties

Soybean leaves were analyzed for their shortwave (350–2,500 nm) reflectance properties using a high-spectral-

resolution ASD FieldSpec® Full-Range spectroradiometer (Analytical Spectral Devices, Boulder, CO, USA). Measurements were made within 30 min of the 59 gas exchange measurements made on the Pana and Dwight genotypes. In addition, spectral measurements were made on 108 plants from the other 9 genotypes (Table 1). Our objective was to calibrate the spectral models using Pana and Dwight, and apply the resulting models to spectral measurements from the remaining genotypes. Genotype is not in and of itself a unit of replication or analysis in this study and data from all genotypes were pooled for most analyses. All measurements were made on the leaf adaxial surface using a leaf-clip assembly attached to a plant probe with an internal, calibrated light source. The relative reflectance of each leaf was determined from the measurement of leaf radiance divided by the radiance of a 92.5–99.5 % reflective white standard (Spectralon,¹ Labsphere Inc., North Dutton, NH, USA), measured every 3rd spectral collection. Each leaf reflectance measurement required less than 5 s. Prior to each spectral measurement we measured leaf temperature on the leaf adaxial side using an infrared thermometer (Agri-Therm III, Everest Interscience, Inc., Tucson, AZ). Three leaves per genotype per treatment were measured, and the average spectral data of three leaves were then used for statistical analysis. For leaves with a paired gas exchange measurement, the collection of reflectance and gas exchange were separated by no more than 15–30 min.

Based on 1-nm bandwidths interpolated from the spectroradiometer data, we calculated PRI according to Gamon et al. (1997):

$$PRI = \frac{R_{531} - R_{570}}{R_{531} + R_{570}}$$

¹ <http://www.labsphere.com/products/reflectance-standards-and-targets/reflectance-targets/spectralon-targets.aspx>.

where R is reflectance and subscripts refer to wavelengths in nm. In order to avoid negative values of PRI , values were scaled as (Letts et al. 2008):

$$sPRI = \frac{PRI + 1}{2}$$

Chlorophyll index (CI) was calculated according to Gitelson and Merzlyak (1994) as:

$$CI = \frac{R_{750} - R_{705}}{R_{750} + R_{705}}$$

and total chlorophyll content (total chl; $\mu\text{g cm}^{-2}$) was estimated from CI following Richardson et al. (2002).

In addition the spectral vegetation indices (SVIs) above, we calculated leaf nitrogen concentration (%) and leaf mass per area (LMA, g m^{-2} dry weight) on all sample leaves based on spectroscopic models presented in Serbin et al. (2012) and Serbin (2012).

Modeling leaf metabolism using reflectance spectroscopy

We modeled the variation in leaf metabolism, based on coincident variation in optical properties, using a partial least-squares regression (PLSR) modeling approach (Wold et al. 1984; Geladi and Kowalski 1986; Asner et al. 2011; Serbin et al. 2012). The PLSR approach is useful in remote sensing research, particularly leaf spectroscopy, because it facilitates relating a full reflectance spectrum to a response variable of interest, in this case $V_{c,\text{max}}$. To avoid potential overfitting during the PLSR modeling step, we optimized the number of PLSR model components by minimizing the prediction residual sum of squares (PRESS) statistic (Chen et al. 2004). We calculated the PRESS statistic for successive components through an iterative leave-one-out cross-validation (LOO-CV) procedure. Once minimized, we then used the corresponding number of components in the final $V_{c,\text{max}}$ model (Wold et al. 2001; Asner et al. 2011; Serbin et al. 2012). This model was then used to estimate $V_{c,\text{max}}$ on the remaining leaf samples using the original spectral data. The validation statistics were used to determine the precision and accuracy of the estimates from spectroscopy, where the coefficient of determination (r^2) was used to assess the precision of the PLSR model and the residual between calibration and LOO-CV prediction values (root mean square error, RMSE) provides an assessment of model performance (Serbin et al. 2012). The final $V_{c,\text{max}}$ model was then applied to spectra collected from genotypes that did not have concurrent gas exchange measurements.

Statistical analysis

The effect of ozone on spectral properties and soybean seed yield was analyzed by ANOVA (PROC GLM; SAS 9.2,

SAS Institute, Cary, NC) and differences between ambient and elevated ozone were considered significant at $p < 0.10$. Plot mean were used for ANOVA and correlations among parameters. Relationships between spectral indices and estimated leaf biochemical properties and seed yield was assessed by linear regression (PROC REG; SAS 9.2, SAS Institute) using data from all eleven genotypes.

Results

Estimating $V_{c,\text{max}}$ from leaf reflectance spectra

Leaf optical properties for the youngest, fully expanded leaf samples used in the PLSR $V_{c,\text{max}}$ modeling varied significantly within and across the ozone treatments as well as the two genotypes of soybean, Dwight and Pana (Fig. 2). We observed the largest range in reflectance in the near-infrared region (NIR, 750–1,300 nm), however, the coefficient of variation (CV) of reflectance (Fig. 2b) was largest in the visible (VIS, 450–750 nm), followed by the short-wave infrared (SWIR, 1,500–2,500 nm) spectral regions.

During the experiment, leaf temperatures ranged from 25 to 34 °C and $V_{c,\text{max}}$ varied from a minimum of 81 to a maximum value of 264 $\mu\text{mol m}^{-2} \text{s}^{-1}$ for the two genotypes used within the PLSR calibration data (Fig. 3). $V_{c,\text{max}}$ displayed a typical temperature sensitivity and the response to temperature was well described by an Arrhenius relationship (Fig. 3c), resulting in an activation energy near 80 kJ mol^{-1} . The values of $V_{c,\text{max}}$, standardized to a reference temperature of 25 °C ($V_{c,\text{max}}^{25}$), ranged from a minimum of 76.3 $\mu\text{mol m}^{-2} \text{s}^{-1}$ to a peak value of 136.1 $\mu\text{mol m}^{-2} \text{s}^{-1}$, and there was no significant effect of O_3 ($p = 0.154$) or cultivar ($p = 0.901$) on the values of $V_{c,\text{max}}^{25}$.

Despite the variation in $V_{c,\text{max}}$ we observed across the ambient plots and ozone treatments, as well as genotypes, our PLSR model, which was based on leaf reflectance, was able to estimate $V_{c,\text{max}}$ with high accuracy and precision (Fig. 3a, b). The final model did not contain a significant bias and the root mean square error (RMSE) was within 9.4 % of the mean $V_{c,\text{max}}$. We did not observe any significant trends in the residuals with leaf temperature or nitrogen content (product of nitrogen concentration and leaf mass per area, g m^{-2}), which displayed an almost a twofold variation across samples. The PLSR model coefficients (Fig. 2c) showed that the contribution of reflectance to the prediction of $V_{c,\text{max}}$ varied considerably across the spectrum. Strong loadings were observed in the visible spectrum near the chlorophyll absorption features (640–670 nm) and the shoulders of the green reflectance peak (~ 550 nm), as well as the around red-edge (~ 750 nm) region. In the SWIR, we found large model

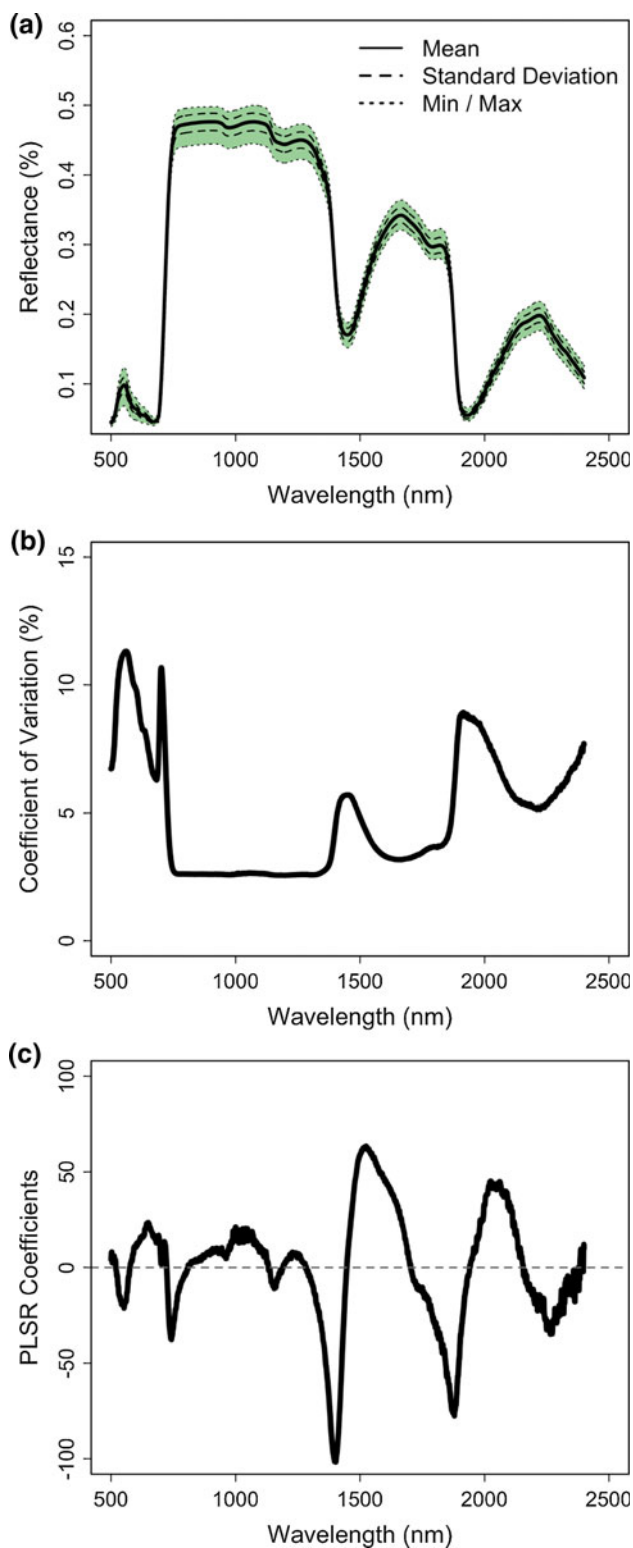


Fig. 2 Mean, \pm one standard deviation, and range in leaf reflectance for the 59 observations (28 Dwight, 31 Pana) with concurrent leaf gas exchange measurements (a). Spectral coefficient of variation (CV) of leaf reflectance (b) and the $V_{c,max}$ PLSR model coefficients by wavelength (c) for the same 61 samples

coefficients (thus strong loadings) near the shoulders of the strong water absorption features ($\sim 1,400$ and $1,900$ nm) as well as near $1,700$ and $2,200$ nm.

Ozone alters leaf spectral properties and seed yield

Across all soybean genotypes, there was a significant effect of elevated ozone concentrations (~ 80 ppb) on soybean leaf properties as measured using spectroscopy (Fig. 4). Leaf N concentration decreased from 3.1 to 2.9 % and total chlorophyll content also decreased from 40 to $37 \mu\text{g cm}^{-2}$. sPRI, an indication of the epoxidation state of xanthophyll pigments, was significantly decreased by elevated ozone (Fig. 4). Contrary to our expectation, leaf level $V_{c,max}$ was unaffected at elevated ozone (Fig. 4). Ozone had a significant detrimental effect on seed yield, reducing production on average by ~ 30 % (Fig. 4).

Relationship between spectral properties and seed yield

There was a significant, positive correlation between leaf N, chlorophyll content, sPRI and seed yield (Fig. 5; Table 2). All three of the leaf level traits were also highly correlated with each another, especially leaf N and total chlorophyll content (Table 2). There was no significant relationship between $V_{c,max}$ and seed yield (Fig. 5; Table 2), and $V_{c,max}$ estimated from spectral data was also not correlated with sPRI or chlorophyll content, suggesting that ozone had differential effects on light harvesting and carbon assimilation.

Discussion

We exposed 11 soybean genotypes to ambient and elevated concentrations of ozone in the field under standard agronomic conditions. Exposure to elevated ozone decreased seed yield by ~ 30 % on average and also impacted leaf level traits assessed from spectral optical properties. Leaf nitrogen, total chlorophyll content, and sPRI were all significantly lower in plants exposed to elevated ozone (Fig. 3). A change in the spectral characteristics of plants exposed to elevated ozone has been previously documented (Williams and Ashenden 1992; Rudorff et al. 1996; Campbell et al. 2007; Meroni et al. 2009), and the decrease in PRI with exposure to elevated ozone is consistent with previous studies of soybeans (Gray et al. 2010). In our study, reduced values of PRI indicate the increased protective dissipation of excess energy as a response to elevated ozone concentrations by sensitive plants (Guidi et al. 1997; Carrasco-Rodriguez and del Valle-Tascon 2001).

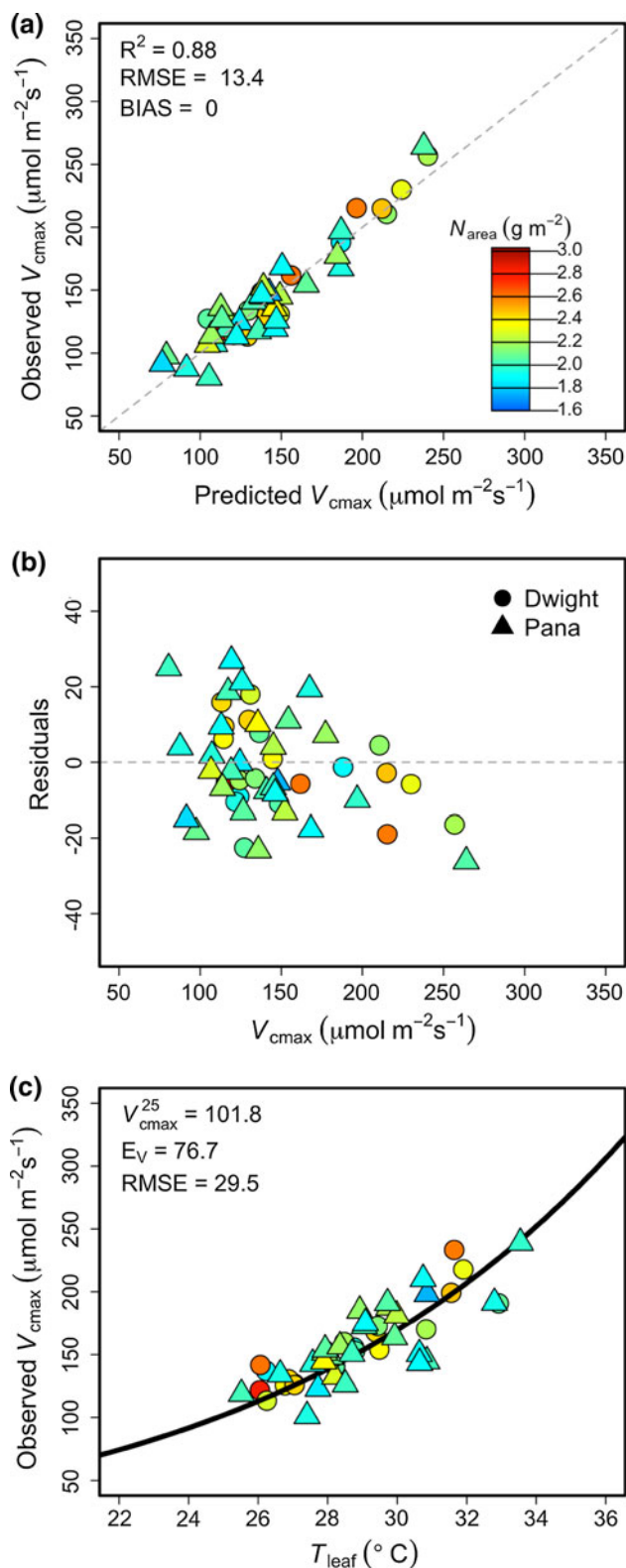


Fig. 3 Observed versus PLSR predicted $V_{c,max}$ (a) and corresponding model residuals (b) for the 61 samples across the Dwight and Pana cultivars. Observed $V_{c,max}$ values were adjusted prior to model fitting to match the temperature of each leaf during spectral correction using an Arrhenius temperature response function (c) derived from the leaf gas exchange samples

The decrease in chlorophyll and nitrogen content at elevated ozone is also consistent with previous studies (Reid et al. 1998; Shrestha and Grantz 2005) and consistent with decreased leaf absorbance measured at SoyFACE (Betzelberger et al. 2012). While another previous study at SoyFACE did not find a significant effect of elevated ozone (82.5 ppb) on chlorophyll content, it did report transcriptional evidence for increased turnover of chlorophyll (Gillepsie et al. 2012).

We assessed the potential for using spectral data to estimate $V_{c,max}$ in soybean plants exposed to elevated ozone. Our PLSR modeling approach was previously developed to estimate photosynthetic metabolism in trembling aspen (*Populus tremuloides*) and eastern cottonwood (*Populus deltoides*; Serbin et al. 2012), which we have now extended across diverse genotypes of soybean. Our PLSR model provided very accurate estimates of $V_{c,max}$ (Fig. 3a), based on the strong relationship between leaf metabolism and variations in leaf optical properties across the Vis–NIR–SWIR spectral region (Fig. 2). Only a few studies have explored the potential to estimate photosynthetic capacity, expressed as $V_{c,max}$, using leaf optical properties (Wang et al. 2008; Doughty et al. 2011; Dillen et al. 2012; Serbin et al. 2012), and to our knowledge no others have explored this potential on environmentally stressed plants. Importantly, the relationship between leaf reflectance and $V_{c,max}$ was strong despite the large variation in leaf morphology, chemistry, measurement temperature, and environmental stress, as well as across genotypes of soybean. In addition, the spectral regions of high importance to the prediction of $V_{c,max}$ (i.e., large model coefficients, Fig. 2c) align closely with those shown in our previous work (Serbin et al. 2012) and generally lie within the pigment absorption features, as well as those related to foliar nitrogen, structure, and Rubisco absorption (Curran 1989; Elvidge 1990; Kokaly et al. 2009; Ustin et al. 2009). Dillen et al. (2012) also found that the red-edge region of a leaf spectrum (~ 750 nm) was a good predictor of $V_{c,max}$, but found accuracies lower than those shown here or in Serbin et al. (2012). This is likely due to the differences in leaf temperature during gas exchange and spectral measurements, which we have found to be necessary to accurately relate leaf optical properties to leaf metabolism.

We did not detect an effect of ozone on $V_{c,max}$ in this study (Fig. 4). This was unexpected given the ozone-induced decreases in leaf N percentage, chlorophyll content, and sPRI. However, the season-long average ozone concentration in the ambient air was 44 nL L^{-1} ($\text{AOT}_{40} = 4.92 \text{ ppm h}$), which exceeds the minimum threshold for damage in soybean (Mills et al. 2007). While we cannot rule out that ambient ozone concentrations caused reductions in potential $V_{c,max}$, we did expect to see a greater decrease in $V_{c,max}$ in the elevated ozone plots.

Fig. 4 Variation in leaf traits and seed yield of 11 soybean genotypes exposed to ambient (white boxes) and elevated (gray boxes) ozone concentrations. The box plots display the median for each trait by group (dark horizontal line), the interquartile range (IRQ, boxes), the range (whiskers), and the extreme observations (black dots). Traits include leaf nitrogen percentage (Leaf N %), maximum carboxylation rate of Rubisco ($V_{c,max}$), scales photochemical reflectance index (sPRI), total chlorophyll content (Total Chl), and seed yield. The mean square error (MSE) from the analysis of variance and level of significance is also shown. * $p < 0.10$, ** $p < 0.05$, *** $p < 0.01$

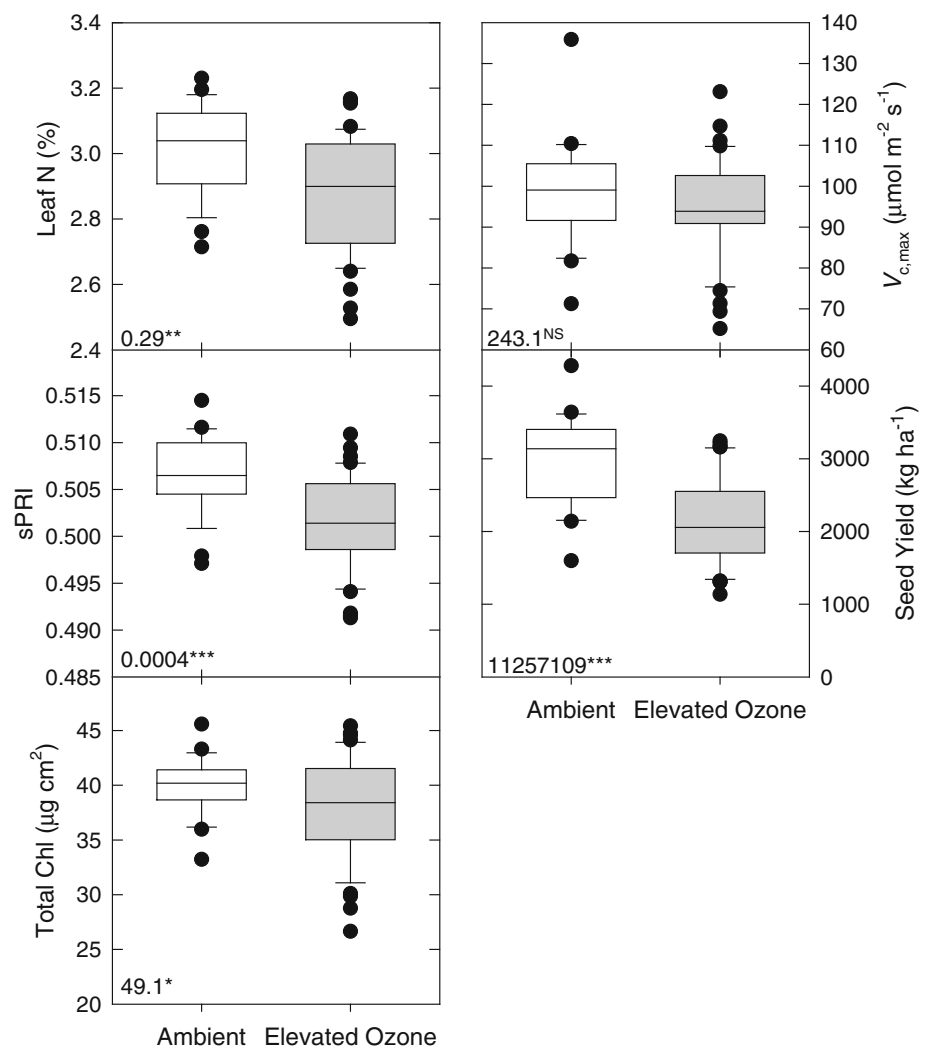


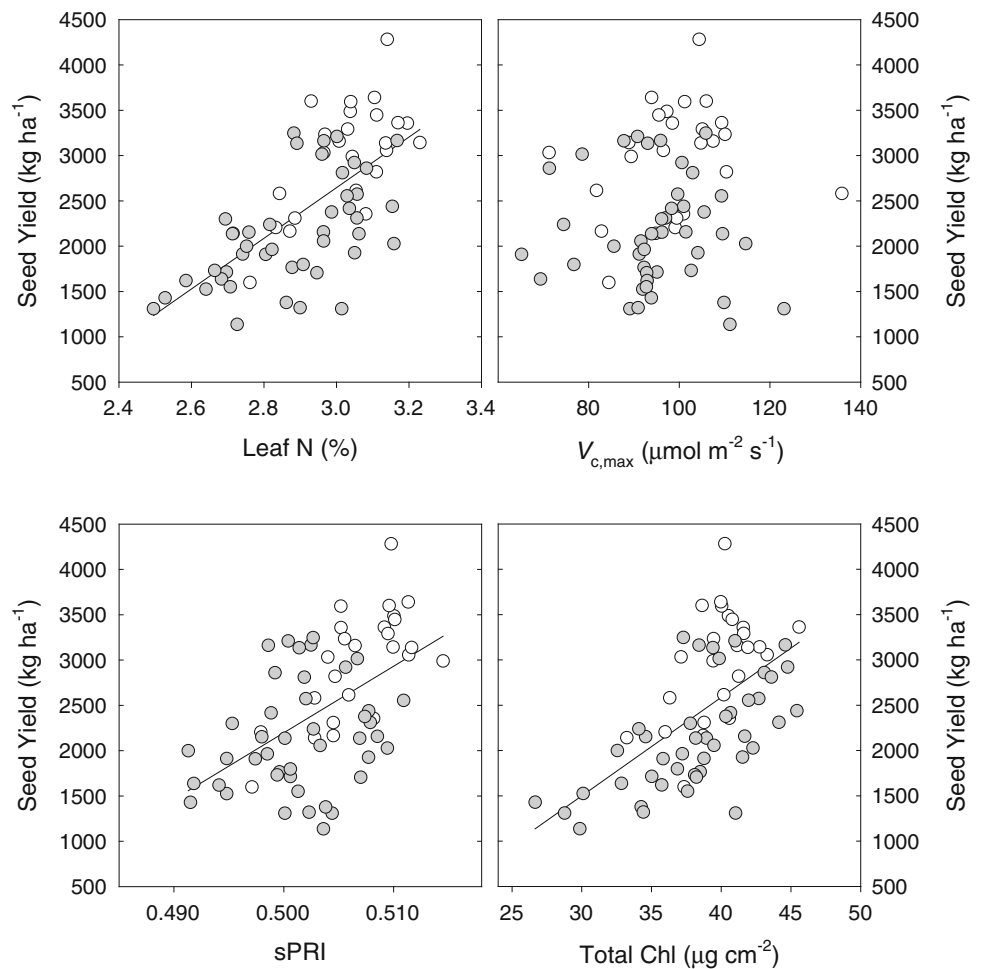
Table 2 Correlation matrix (Pearson correlation coefficient— r , statistical significance— p) of leaf properties derived from spectral data and seed yield measured on 11 cultivars of soybean exposed to ambient and elevated ozone. $N = 68$. See text for abbreviations

| | $V_{c,max}$ | sPRI | Total Chl | Yield |
|-------------|----------------|-----------------|-----------------|-----------------|
| Leaf N (%) | 0.1060, 0.1520 | 0.5348, <0.0001 | 0.8864, <0.0001 | 0.6718, <0.0001 |
| $V_{c,max}$ | | -0.0489, 0.6228 | 0.0376, 0.6117 | 0.1125, 0.3609 |
| sPRI | | | 0.5465, <0.0001 | 0.5444, <0.0001 |
| Total Chl | | | | 0.5928, <0.0001 |

However, previous studies of soybean and wheat exposed to elevated ozone concentration in field conditions have demonstrated that declines in $V_{c,max}$ in ozone-exposed leaves are coincident with late-season acceleration in senescence (Morgan et al. 2004; Feng et al. 2011). In previous studies, decreases in $V_{c,max}$ in soybean plants exposed to elevated ozone were only apparent late in the growing season when leaves were ~25–30 days old (Morgan et al. 2004). In this study, we may not have sampled leaves at a time when changes in $V_{c,max}$ would be

expected. Morgan et al. (2004) also reported a significant decrease in photochemical quenching of soybean leaves that preceded changes in $V_{c,max}$ and photosynthetic CO_2 assimilation. Therefore, we believe it possible that under chronic ozone exposure, changes to the light harvesting complexes and thermal dissipation of energy precede changes to Rubisco (i.e., $V_{c,max}$), although this is the opposite of the sequence of events following acute ozone exposure documented in other species (Farage et al. 1991). Certainly more frequent spectral characterization of both

Fig. 5 Correlation between soybean seed yield and leaf properties estimated from spectral data collected from 11 soybean genotypes. Each point represents the plot mean for each genotype with *open circles* showing ambient plots and *gray circles* showing elevated ozone plots. Correlation information is provided in Table 2. See the legend of Fig. 2 for abbreviations



$V_{c,max}$ over the course of the growing season would improve understanding of the timing of ozone effects on different photosynthetic processes, as well as other environmental stressors. Other measurements, for example of J_{max} , the maximum electron transport capacity for the regeneration of RuBP, may further elucidate the temporal patterns of response of soybean to elevated ozone.

In the current study, leaf N content, total chlorophyll content, and sPRI were significantly correlated to soybean yield and yield loss to ozone (Fig. 5), supporting the use leaf reflectance measurements for screening for ozone tolerance in a larger collection of soybean germplasm. Although genetic variation in ozone tolerance has been reported in soybean (Betzberger et al. 2010; Burkey and Carter 2009), snap bean (Flowers et al. 2007), rice (Frei et al. 2008, 2010), and wheat (Picchi et al. 2010), there has been little effort in industry to begin to breed crops for ozone tolerance (Ainsworth et al. 2008; Booker et al. 2009). This may be in part because ozone is a dynamic pollutant, and not always present in the growing environment. It is also because it has been difficult to identify consistent physiological markers of ozone tolerance.

Remote or near-remote sensing of leaf optical properties is a very promising, rapid phenotyping technique as a number of physiological traits can be inferred by correlation with leaf optical properties (Montes et al. 2007; Kokaly et al. 2009; Asner et al. 2011). Here, we show that $V_{c,max}$ can be accurately predicted from leaf reflectance spectra, and although it was not correlated with ozone tolerance at the time we took our measurements, other inferred leaf properties were correlated with ozone tolerance, as ultimately measured by seed yield. Therefore, combining the phenotyping methods used here with high-throughput genotyping methods may be a promising approach for elucidating the basis for ozone tolerance in sensitive crops.

Acknowledgments We thank Chris Montes, Kannan Puthuval, and David Drag for managing SoyFACE, and Donald Ort for facilitating research. Chris Montes, Joe Sullivan, and Amy Betzelberger assisted with measurements of leaf optical properties and gas exchange. This study was supported in part by the Agriculture and Food Research Initiative competitive grant no. 2010-65114-20355 from the USDA National Institute of Food and Agriculture to E.A.A., NASA Earth and Space Science Fellowship NNX08AV07H to S.P.S. and NASA HypIRI Preparatory Grant NNX10AJ94G to P.A.T.

References

- Ainsworth EA, Rogers A, Leakey ADB (2008) Targets for crop biotechnology in a future high-CO₂ and high-O₃ world. *Plant Physiol* 147:13–19
- Ainsworth EA, Yendrek CR, Sitch S, Collins WJ, Emberson LD (2012) The effects of tropospheric ozone on net primary productivity and implications for climate change. *Annu Rev Plant Biol* 63:637–661
- Ardia D (2009) DEoptim: differential evolution optimization in R. R package, version 1.3-3. <http://CRAN.R-project.org/package=DEoptim>
- Ashmore MR (2005) Assessing the future global impacts of ozone on vegetation. *Plant Cell Environ* 28:949–964
- Asner GP, Martin RE, Knapp DE, Tupayachi R, Anderson C, Carranza L, Martinez P, Houcheime M, Sinca F, Weiss P (2011) Spectroscopy of canopy chemicals in humid tropical forests. *Remote Sens Environ* 115:3587–3598
- Babar MA, Reynolds MP, Van Ginkel M, Klatt AR, Raun WR, Stone ML (2006) Spectral reflectance to estimate genetic variation for in-season biomass, leaf chlorophyll and canopy temperature in wheat. *Crop Sci* 46:1046–1057
- Baldocchi DD, Wilson KB (2001) Modeling CO₂ and water vapor exchange of a temperate broadleaved forest across hourly to decadal time scales. *Ecol Model* 142:155–184
- Bernacchi CJ, Singaas EL, Pimentel C, Portis AR, Long SP (2001) Improved temperature response functions for models of Rubiscolimited photosynthesis. *Plant Cell Environ* 24:253–259
- Betzberger AM, Gillespie KM, McGrath JM, Koester RP, Nelson RL, Ainsworth EA (2010) Effects of chronic elevated ozone concentration on antioxidant capacity, photosynthesis and seed yield of 10 soybean cultivars. *Plant Cell Environ* 33:1569–1581
- Betzberger AM, Yendrek CR, Sun J, Leisner CP, Nelson RL, Ort DR, Ainsworth EA (2012) Ozone exposure response for U.S. soybean cultivars: linear reductions in photosynthetic potential, biomass, and yield. *Plant Physiol* 160:1827–1839
- Biswas DK, Xu H, Li YG, Liu MZ, Chen YH, Sun JZ, Jiang GM (2008) Assessing the genetic relatedness of higher ozone sensitivity of modern wheat to its wild and cultivated progenitors/relatives. *J Exp Bot* 59:951–963
- Booker F, Muntifering R, McGrath M, Burkey K, Decoteau D, Fiscus E, Manning W, Krupa S, Chappelka A, Grantz D (2009) The ozone component of global change: potential effects on agricultural and horticultural plant yield, product quality and interactions with invasive species. *J Integr Plant Biol* 51:337–351
- Burkey KO, Carter TE (2009) Foliar resistance to ozone injury in the genetic base of U.S. and Canadian soybean and prediction of resistance in descendent cultivars using coefficient of parentage. *Field Crops Res* 111:207–217
- Campbell PKE, Middleton EM, McMurtrey JE, Corp LA, Chappelle EW (2007) Assessment of vegetation stress using reflectance or fluorescence measurements. *J Environ Qual* 36:832–845
- Carrasco-Rodriguez JL, del Valle-Tascon S (2001) Impact of elevated ozone on chlorophyll *a* fluorescence in field-grown oat (*Avena sativa*). *Environ Exp Bot* 45:133–142
- Castagna A, Nali C, Ciompi S, Lorenzini G, Soldani GF, Ranieri A (2001) Ozone exposure affects photosynthesis of pumpkin (*Cucurbita pepo*) plants. *New Phytol* 152:223–229
- Chen JM, Liu J, Cihlar J, Goulden ML (1999) Daily canopy photosynthesis model through temporal and spatial scaling for remote sensing applications. *Ecol Model* 124:99–119
- Chen S, Hong X, Harris CJ, Sharkey PM (2004) Sparse modeling using orthogonal forest regression with PRESS statistic and regularization. *IEEE T Syst Man Cyb* 34:898–911
- Coops NC, Hilker T, Hall FG, Nichol CJ, Drolet GG (2010) Estimation of light-use efficiency of terrestrial ecosystem from space: a status report. *Bioscience* 60:788–797
- Curran PJ (1989) Remote-sensing of foliar chemistry. *Remote Sens Environ* 30:271–278
- Dillaway DN, Kruger EL (2010) Thermal acclimation of photosynthesis: a comparison of boreal and temperate tree species along a latitudinal transect. *Plant Cell Environ* 33:888–899
- Dillen SY, de Beeck MO, Hufkens K, Buonanduci M, Phillips NG (2012) Seasonal patterns of foliar reflectance in relation to photosynthetic capacity and color index in two co-occurring tree species, *Quercus rubra* and *Betula papyrifera*. *Agric For Meteorol* 160:60–68
- Doughty C, Asner G, Martin R (2011) Predicting tropical plant physiology from leaf and canopy spectroscopy. *Oecologia* 165:289–299
- Elvidge CD (1990) Visible and near-infrared reflectance characteristics of dry plant materials. *Int J Remote Sens* 11:1775–1795
- Farage PK, Long SP (1999) The effects of O₃ fumigation during leaf development on photosynthesis of wheat and pea: an in vivo analysis. *Photosyn Res* 59:1–7
- Farage PK, Long SP, Lechner EG, Baker NR (1991) The sequence of change within the photosynthetic apparatus of wheat following short-term exposure to ozone. *Plant Physiol* 95:529–535
- Farquhar GD, von Caemmerer S (1982) Modeling photosynthetic response to environmental conditions. In: Lange OL, Nobel PS, Osmond CB, Ziegler H (eds) *Encyclopedia of plant physiology*, vol 12B. Springer-Verlag, Berlin, pp 549–587
- Farquhar GD, von Caemmerer S, Berry JA (1980) A biochemical model of photosynthetic CO₂ assimilation in leaves of C3 species. *Planta* 149:78–90
- Feng ZZ, Pang J, Kobayashi K, Zhu JG, Ort DR (2011) Differential responses in two varieties of winter wheat to elevated ozone concentration under fully open-air field conditions. *Global Change Biol* 17:580–591
- Fiscus EL, Booker FL, Burkey KO (2005) Crop responses to ozone: uptake, modes of action, carbon assimilation and partitioning. *Plant, Cell Environ* 28:997–1011
- Flowers MD, Fiscus EL, Burkey KO, Booker FL, Dubois JJB (2007) Photosynthesis, chlorophyll fluorescence, and yield of snap bean (*Phaseolus vulgaris* L.) genotypes differing in sensitivity to ozone. *Environ Exp Bot* 61: 190–198
- Frei M, Tanaka JP, Wissuwa M (2008) Genotypic variation in tolerance to elevated ozone in rice: Dissection of distinct genetic factors linked to tolerance mechanisms. *J Exp Bot* 59: 3741–3752
- Frei M, Tanaka JP, Chen CP, Wissuwa M (2010) Mechanisms of ozone tolerance in rice: characterization of two QTLs affecting leaf bronzing by gene expression profiling and biochemical analyses. *J Exp Bot* 61:1405–1417
- Fuhrer J, Skärby L, Ashmore MR (1997) Critical levels for ozone effects on vegetation in Europe. *Environ Pollut* 1–2:91–106
- Fumigalli I, Gimeno BS, Velissariou D, De Temmerman L, Mills G (2001) Evidence of ozone-induced adverse effects on crops in the Mediterranean region. *Atmos Environ* 35:2583–2587
- Furbank RT, Tester M (2011) Phenomics – technologies to relieve the phenotyping bottleneck. *Trends Plant Sci* 16:635–644
- Gamon JA, Peñuelas J, Field CB (1992) A narrow-waveband spectral index that tracks diurnal changes in photosynthetic efficiency. *Remote Sens Environ* 41:35–44
- Gamon JA, Field CB, Goulden ML, Griffin KL, Hartley AE, Joel G, Peñuelas J, Valentini R (1995) Relationships between NDVI, canopy structure, and photosynthesis in 3 Californian vegetation types. *Ecol Appl* 5:28–41

- Gamon JA, Serrano L, Surfus JS (1997) The photochemical reflectance index: an optical indicator of photosynthetic radiation use efficiency across species, functional types, and nutrient levels. *Oecologia* 112:492–501
- Geladi P, Kowalski BR (1986) Partial least-squares regression—a tutorial. *Anal Chim Acta* 185:1–17
- Gillespie KM, Xu FX, Richter KT, McGrath JM, Markelz RJC, Ort DR, Leakey ADB, Ainsworth EA (2012) Greater antioxidant and respiratory metabolism in field-grown soybean exposed to elevated O₃ under both ambient and elevated CO₂. *Plant, Cell Environ* 35:169–184
- Gitelson A, Merzlyak MN (1994) Quantitative estimation of chlorophyll a using reflectance spectra—experiments with autumn chestnut and maple leaves. *J Photochem Photobiol* 22:247–252
- Gitelson AA, Vina A, Arkebauer TJ, Rundquist DC, Keydan G, Leavitt B (2003) Remote estimation of leaf area index and green leaf biomass in maize canopies. *Geophys Res Lett* 30:4
- Grace J, Nichol C, Disney M, Lewis P, Quaife T, Bowyer P (2007) Can we measure terrestrial photosynthesis from space directly, using spectral reflectance and fluorescence? *Global Change Biol* 13:1484–1497
- Gray SB, Dermody O, De Lucia EH (2010) Spectral reflectance from a soybean canopy exposed to elevated CO₂ and O₃. *J Exp Bot* 61:4413–4422
- Guidi L, Nali C, Ciompi S, Lorenzini G, Franco G (1997) The use of chlorophyll fluorescence and leaf gas exchange as methods for studying the different responses to ozone of two bean cultivars. *J Exp Bot* 48:173–179
- Heagle AS, Letchworth MB (1982) Relationships among injury, growth and yield responses of soybean cultivars exposed to ozone at different light intensities. *J Environ Qual* 11:690–694
- Kattge J, Knorr W (2007) Temperature acclimation in a biochemical model of photosynthesis: a reanalysis of data from 36 species. *Plant, Cell Environ* 30:1176–1190
- Kokaly RF, Asner GP, Ollinger SV, Martin ME, Wessman CA (2009) Characterizing canopy biochemistry from imaging spectroscopy and its application to ecosystem studies. *Remote Sens Environ* 113:S78–S91
- Letts MG, Phelan CA, Johnson DRE, Rood SB (2008) Seasonal photosynthetic gas exchange and leaf reflectance characteristics of male and female cottonwoods in a riparian woodland. *Tree Physiol* 28:1037–1048
- Long SP, Bernacchi CJ (2003) Gas exchange measurements, what can they tell us about the underlying limitations to photosynthesis? Procedures and sources of error. *J Exp Bot* 54:2393–2401
- Medlyn BE, Dreyer E, Ellsworth D, Forstreuter M, Harley PC, Kirschbaum MUF, Le Roux X, Montpied P, Strassmeyer J, Walcroft A et al (2002) Temperature response of parameters of a biochemically based model of photosynthesis. II. A review of experimental data. *Plant, Cell Environ* 25:1167–1179
- Medvigy D, Wofsy SC, Munger JW, Hollinger DY, Moorcroft PR (2009) Mechanistic scaling of ecosystem function and dynamics in space and time: ecosystem Demography model version 2. *J Geophys Res* 114:G01002
- Meroni M, Panigada C, Rossini M, Picchi V, Cogliati S, Colombo R (2009) Using optical remote sensing techniques to track the development of ozone-induced stress. *Environ Pollut* 157:1413–1420
- Mills G, Buse A, Gimeno B, Bermejo V, Holland M, Emberson L, Pleijel H (2007) A synthesis of AOT40-based response functions and critical levels of ozone for agricultural and horticultural crops. *Atmos Environ* 41:2630–2643
- Mills G, Hayes F, Simpson D, Emberson L, Norris D, Harmens H, Büker P (2011) Evidence of widespread effects of ozone on crops and (semi-) natural vegetation in Europe (1990–2006) in relation to AOT40- and flux-based risk maps. *Global Change Biol* 17:592–613
- Montes JM, Melchinger AE, Reif JC (2007) Novel throughput phenotyping platforms in plant genetic studies. *Trends Plant Sci* 12:433–436
- Morgan PB, Bernacchi CJ, Ort DR, Long SP (2004) An in vivo analysis of the effect of season-long open-air elevation of ozone to anticipated 2050 levels on photosynthesis in soybean. *Plant Physiol* 135:2348–2357
- Myneni RB, Williams DL (1994) On the relationship between FAPAR and NDVI. *Remote Sens Environ* 49:200–211
- Ollinger SV (2011) Sources of variability in canopy reflectance and the convergent properties of plants. *New Phytol* 189:375–394
- Osborne SL, Schepers JS, Francis DD, Schlemmer MR (2002) Use of spectral radiance to estimate in-season biomass and grain yield in nitrogen- and water-stressed corn. *Crop Sci* 42:165–171
- Peñuelas J, Filella I, Biel C, Serrano L, Save R (1993) The reflectance at the 950–970 nm region as an indicator of plant water status. *Int J Remote Sens* 14:1887–1905
- Peñuelas J, Filella I, Gamon JA (1995) Assessment of photosynthetic radiation-use efficiency with spectral reflectance. *New Phytol* 131:291–296
- Picchi V, Iriti M, Quaroni S, Saracchi M, Viola P, Faoro F (2010) Climate variations and phenological stages modulate ozone damages in field-grown wheat. A three-year study with eight modern cultivars in Po Valley (Northern Italy). *Agricul Ecosys Environ* 135:310–317
- Price KV, Storn RM, Lampinen JA (2006) *Differential evolution: a practical approach to global optimization*. Springer, New York
- Ranieri A, Giuntini D, Ferraro F, Nali C, Baldan B, Lorenzini G, Soldatini GF, Soldatini F (2001) Chronic ozone fumigation induces alterations in thylakoid functionality and composition in two poplar clones. *Plant Physiol Biochem* 39:999–1008
- Reid CD, Fiscus EL, Burkey KO (1998) Combined effects of chronic ozone and elevated CO₂ on Rubisco activity and leaf components in soybean (*Glycine max*). *J Exp Bot* 49:1999–2011
- Richardson AD, Duigan SP, Berlyn GP (2002) An evaluation of noninvasive methods to estimate foliar chlorophyll content. *New Phytol* 153:185–194
- Rogers A, Allen DJ, Davey PA, Morgan PB, Ainsworth EA, Bernacchi CJ, Cornic G, Dermody OC, Heaton EA, Mahoney J et al (2004) Leaf photosynthesis and carbohydrate dynamics of soybean grown throughout their life-cycle under free-air carbon dioxide enrichment. *Plant Cell Environ* 28:449–458
- Rudorff BFT, Mulchi CL, Daughtry CST, Lee EB (1996) Growth and radiation use efficiency of wheat and corn grown under elevated ozone and carbon dioxide atmospheres. *Remote Sens Environ* 55:163–173
- Serbin SP (2012) Spectroscopic determination of leaf nutritional, morphological, and metabolic traits. Dissertation, University of Wisconsin - Madison, Madison, Wisconsin, Ph.D
- Serbin SP, Dillaway DN, Kruger EL, Townsend PA (2012) Leaf optical properties reflect variation in photosynthetic metabolism and its sensitivity to temperature. *J Exp Bot* 63:489–502
- Shrestha A, Grantz DA (2005) Ozone impacts on competition between tomato and yellow nutsedge: above- and below-ground effects. *Crop Sci* 45:1587–1595
- Tuberosa R (2012) Phenotyping for drought tolerance of crops in the genomics era. *Front Physiol* 3:347. doi:10.3389/fphys.2012.00347
- Ustin SL, Gitelson AA, Jacquemoud S, Schaepman M, Asner GP, Gamon JA, Zarco-Tejada P (2009) Retrieval of foliar information about plant pigment systems from high resolution spectroscopy. *Remote Sens Environ* 113:S67–S77

- Van Dingenen R, Dentener FJ, Raes F, Krol MC, Emberson L, Cofala J (2009) The global impact of ozone on agricultural crop yields under current and future air quality legislation. *Atmos Environ* 43:604–618
- Wang Q, Iio A, Kakubari Y (2008) Broadband simple ratio closely traced seasonal trajectory of canopy photosynthetic capacity. *Geophys Res Letters* 35:L07401
- Williams JH, Ashenden TW (1992) Differences in the spectral characteristics of white clover exposed to gaseous pollutants and acid mist. *New Phytol* 120:69–75
- Wold S, Ruhe A, Wold H, Dunn WJ (1984) The collinearity problem in linear-regression—the partial least-squares (PLS) regression approach to generalized inverses. *Siam J Sci Stat Comp* 5:735–743
- Wold S, Sjostrom M, Eriksson L (2001) PLS-regression: a basic tool of chemometrics. *Chemometr Intell Lab* 58:109–130